

Dimensioning of TRC structures

PROF. DR.-ING. J. HEGGER, DIPL.-ING. M. ZELL, DIPL.-ING. S. VOSS
Institute of Structural Concrete, RWTH Aachen University, Germany

Abstract

Textile reinforced concrete (TRC) is a suitable composite material for the production of thin, lightweight elements such as façade panels. Recently various projects have been realised using textile-reinforced elements. For the effective and efficient development and production of TRC elements the availability of dimensioning methods and design equations is vital. The established and well-known design methods for ordinary steel-reinforced concrete cannot be applied to TRC structures. Due to differences in bond performance and in material properties, the load-bearing behaviour of TRC differs significantly from that of steel-reinforced concrete. As a result extensive investigations have been carried out in which varying textile properties and different types of loading (tension, bending and shear) were considered. Based on the results of these experimental and theoretical investigations, adequate design methods for tension, bending and shear loading have been derived for the dimensioning of TRC structures.

Introduction

The use of high-performance fibres as reinforcement for concrete members enables the production of durable and thin lightweight elements with a high potential for economic savings. These advantages, together with the wide range of design options for architects, have rendered glassfibre-reinforced concrete (GFRC) a widespread building material. As the fibres are not aligned in the direction of forces within a structural member and as the fibres are randomly distributed across the cross-section without orientation, the effectiveness of reinforcement with chopped strands is reduced.

In contrast, textile reinforced concrete (TRC) combines the advantages of both GFRC and ordinary steel-reinforced concrete. The fibre material is placed only where necessary and in the direction of the tensile forces; furthermore no minimum concrete cover is required to protect the reinforcement against corrosion. This leads to a higher utilisation of the reinforcement material and better load-bearing properties of the components. The thickness of a structural member primarily depends on the necessary concrete cover to ensure a proper anchorage of the reinforcement and to avoid a splitting failure.

For a successful application of the construction material TRC, the availability of design methods is a basic requirement. Therefore, extensive experimental test programmes and theoretical investigations have been carried out at RWTH Aachen University with the aim of improving the material properties and to derive adequate design methods. With the results of these investigations, production of the first prototypes was possible. The huge application potential of TRC could be demonstrated with the production of thin façade elements of only 25 mm thickness^[1] and a slender diamond-lattice grid^[2].

Materials

The composite material TRC consists of a textile reinforcement embedded in a fine-grained concrete matrix. Generally, the textile reinforcement is a two-dimensional fabric or a three-dimensional spacer fabric. In Table 1 the properties of the fabrics used for the investigations in this paper are presented. These fabrics were produced from alkali-resistant (AR)-glassfibre or carbon rovings, both having a cross-sectional area of 0.89 mm². The AR-glassfibre rovings were produced at Saint Gobain Vetrotex and the carbon rovings by Tenax Fibers.

Name	Material	Filament number	Filament diameter [μm]	Mesh size [mm]	Cross-sectional area [mm ² /m]	Tensile strength [MPa]	
						0° direction	90° direction
MAG-07-03	AR-glass	1300	29	8 × 8	107	848	715
MAG-04-03	Carbon	24 000	7	8 × 8	107	1121	1556
MAG-05-03	Carbon	24 000	7	16 × 16	53	1328	1608

Table 1: Properties of the textile reinforcement

To measure the tensile strength of the fabrics in the 0° and 90° direction in tensile tests, 125 mm long segments of the rovings were taken from the fabrics. In Reference [3] this test method is described in detail. The strength of the rovings is much lower than the strength of the single filaments, amounting to about 1120 MPa for the AR-glass filament and 3980 MPa for the carbon filament. The reasons for this are, for example, the damage to the roving during the textile production process and the non-uniform loading of the filaments due to their waviness.

The properties of the textile reinforcement lead to special demands on the concrete mixture, especially with regard to the rheological properties. Based on these requirements a fine-grained concrete was developed^[4]. The concrete has a compressive strength of about 85 MPa and a tensile strength of 4.4 MPa and is characterised by a very ductile behaviour compared to normal concrete. Young's modulus of 34 000 MPa is lower and the strain at compression failure of about 5‰ is higher compared to normal concrete.

Tensile strength of the component

Previous investigations have shown that with the composite material TRC the tensile strength of the filaments cannot be fully utilised. The main reason for this is the decreasing bond performance from the outer filaments towards the inner core of the roving. Several models have been established taking this effect into consideration. According to Ohno and Hannant^[5] the cross-sectional area of the roving is subdivided into core filaments and sleeve filaments. Based on the results of tensile tests on TRC elements^[6] a factor k_1 for the efficiency was determined. This factor is calculated from the ratio between the measured average strength of the reinforcement embedded in the concrete σ_{\max} and the tensile strength of the filament f_{filament} :

$$k_1 = \frac{\sigma_{\max}}{f_{\text{filament}}} \quad (1)$$

The efficiency is influenced by the bond properties of the rovings, therefore it is also affected by the filament diameter, the type of the binding and the roving thickness. These parameters affect the roving geometry and the penetration of the matrix into the roving. In Table 2 factor k_1 is given as a mean value of at least six single tests. It is obvious that the efficiency of the AR-glassfibre fabric is about double the efficiency of the carbon fabrics. The different bond properties of the fibre materials are a product of different filament diameters and can be observed in the prevailing failure mode of the tensile tests. While the AR-glassfibre filaments fail near the main crack, the carbon rovings are pulled out of the transfer length.

Name	k_1
MAG-07-03	0.42 (AR-glassfibre)
MAG-04-03	0.20 (carbon)
MAG-05-03	0.25 (carbon)

Table 2: Efficiency factor k_1

In addition, the tensile strength of the component is influenced by lateral tensile stresses as biaxial tensile tests on TRC discs revealed. The cracking of the concrete along the reinforcement leads to damage to the rovings and causes a decreasing strength of the component^[7]. Another very important effect is the alignment of the reinforcement in respect of the load direction. The deviating direction of loading and reinforcement leads to significant losses of tensile strength as can be seen in Fig. 1, where the ultimate loads of tensile tests are given for different orientations α of the fabrics.

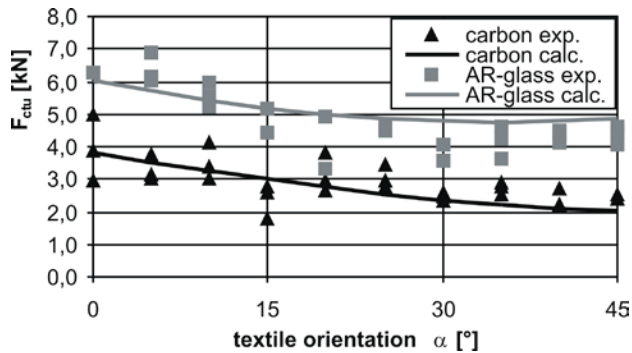


Figure 1: Effect of textile orientation on tensile capacity

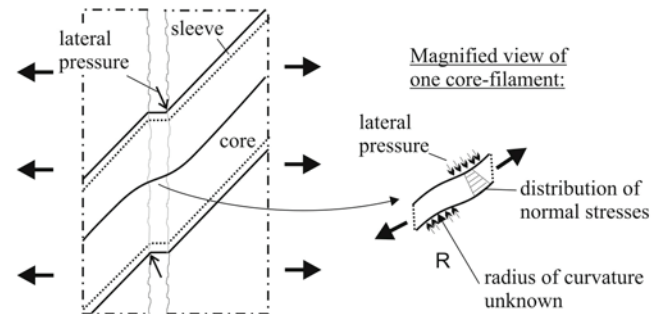


Figure 2: Crack edge with inclined roving

The main effects responsible for this loss of strength are the lateral pressure and the bending stresses of the filaments at the crack edges (Fig. 2). A detailed description of these effects is given in Reference [8]. Based on these results the assumption has been made that the tensile strength of the reinforcement decreases linearly with an increasing angle α between the direction of tensile force and the direction of alignment of the rovings. This interrelationship is represented by the factor $k_{0,\alpha}$:

$$k_{0,\alpha} = 1 - \frac{\alpha}{90^\circ} \quad (2)$$

Results of other investigations concerning the effects of alignment of the rovings with higher loss of strength are described in References [9] and [10]. However, the strength of the specimens calculated with the factor $k_{0,\alpha}$ is in good agreement with the experimental test results as can be seen in Fig. 1. The non-linear trend of the graph results from the changing reinforcement ratio depending on the angle α . Considering the described effects, the tensile strength of the textile reinforced component F_{ctu} can be calculated as follows:

$$F_{ctu} = A_t \cdot f_t \cdot k_1 \cdot k_{0,\alpha} \cdot k_2 \quad (3)$$

where A_t is the cross-sectional area of the reinforcement

f_t is the tensile strength of the reinforcement

k_1 is the efficiency factor

$k_{0,\alpha}$ is the factor for orientation of the reinforcement

k_2 is the factor for biaxial loading^[7].

Bending capacity

Four-point-bending tests on I-section beams with a length of 1 m were used to determine the bending capacity of TRC elements. These beams are 120 mm high, top and bottom flanges are 110 mm wide and the reinforcement is placed in the centre of the components^[1]. The reinforcement of the flange in the tensile zone was varied between one and three layers of fabric whereas the web was always reinforced with two layers. In order to guarantee the accurate position of the textile reinforcement in the formwork the fabrics were clamped and stretched with a low tensile force before concreting. While the vertical loading was applied with deformation control, the deflections and the strain of the components' tension zone were measured with linear variable differential transducers (LVDTs). In some test series longitudinal forces were added which were generated by hydraulic jacks and were kept constant during the tests.

The resulting tensile strength of the reinforcement σ_{\max} under bending loads can be calculated with the knowledge of the maximum loading, the concrete strain ϵ_c and the stress–strain behaviour of the concrete by variation of the textile strain ϵ_f until the equilibrium of longitudinal forces and bending moments is reached.

According to the tests, the AR-glassfibre reinforcement achieved an average tensile strength of about 410 MPa, nearly independent of the reinforcement ratio (Fig. 3), whereas the calculated ultimate strength of the carbon fabric increased with rising reinforcement ratio. The carbon strength amounted to about 1100 MPa for a beam reinforced with one layer (reinforcement ratio of 1%) and reached about 1400 MPa for a beam reinforced with three layers (reinforcement ratio 1.9%). This may be explained as follows. In general, a higher reinforcement ratio leads to lower crack spacing and more cracks accompanied by larger deflections and increasing curvature of the beam. The latter leads to bigger transversal stresses acting on the roving and, hence, to a better bond performance of the filaments. In the case of the carbon fibres, this effect may superpose the damage due to the transversal action at the crack edges. Furthermore, a higher number of cracks leads to a higher strain of the tensile zone of the beam before the failure occurs. The higher strains of the inner filaments improve the effectiveness. This results in a higher ultimate strength of the carbon fabric under bending loading than in a centric tensile test as can be seen in (Fig. 4), where the ratio between the ultimate strength in the bending and the tensile tests is compared. In the case of AR-glassfibre reinforcement, the damaging effects are more pronounced so that the load-carrying capacity amounts to only about 90% of the strength under centric tensile loading. Due to the increasing transversal action on the filaments, the ratio of the ultimate strength under bending and tensile loading decreases with increasing reinforcement ratio.

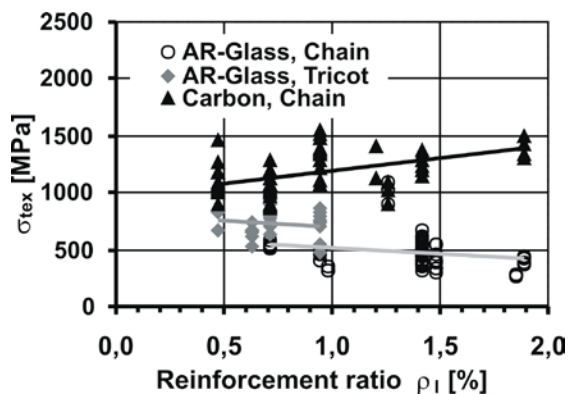


Figure 3: Calculated tensile strength of bending tests

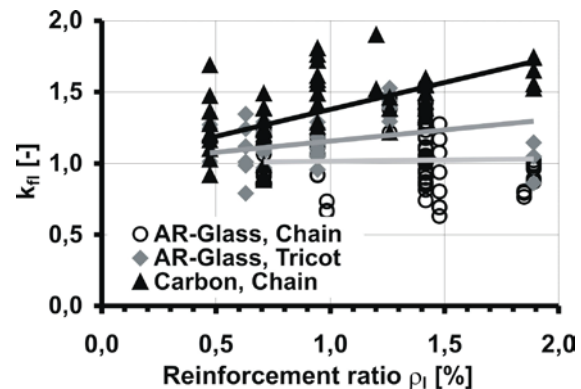


Figure 4: Ratio between tensile strength under bending and tensile loading

For the calculation of the bending capacity the effects due to the transversal action on the reinforcement caused by the curvature (cracking, deflection) of the beam are considered by the factor $k_{fl,\rho}$:

$$\text{AR-glass (chain):} \quad k_{fl,\rho} = 1,0 \quad (4)$$

$$\text{AR-glass (tricot):} \quad k_{fl,\rho} = 1,0 + 0,15 \cdot \rho_l \quad (5)$$

$$\text{Carbon (chain):} \quad k_{fl,\rho} = 1,0 + 0,47 \cdot \rho_l \quad (6)$$

In addition to the reinforcement ratio this factor is influenced by several properties of the reinforcement, e.g. the binding type, the diameter of the roving or an additional impregnation of the fabric. Therefore, in this paper only the results for the fabrics described in Table 1 are given. These may be different for fabrics with other properties.

In accordance with steel-reinforced concrete the bending capacity can be calculated with the knowledge of the tensile strength of the reinforcement F_{ctu} and the inner lever arm z :

$$M_u = k_{fl,\rho} \cdot F_{ctu} \cdot z \quad (7)$$

where $k_{fl,\rho}$ is the factor for bending loading

F_{ctu} is given according to equation (3)

Z is the inner lever arm.

Shear capacity

For the shear tests the same I-section beams were employed that were also used for the bending tests. The main parameter was the reinforcement of the web which was varied along the length of the beam in order to carry out two shear tests with each specimen. First, a four-point bending test was carried out in which the part of the web with lower reinforcement ratio failed. After that the remaining part of the beam with the higher shear reinforcement ratio was tested in a three-point bending test.

The test programme included tests with varying shear reinforcement ratios and fibre materials as well as tests with additional longitudinal force. In addition, in one test series the effect of the horizontal rovings parallel to the beam axis in the web was investigated on beams that were reinforced with and without horizontal rovings.

An important issue was the accurate determination of the deformation of the shear area with a photogrammetry measurement system (Fig. 5)^[12]. In particular the relative movement of the shear crack edges was of major interest. With these data the effect of the angular change of the shear reinforcement α and the effect of friction forces at the shear crack edges were evaluated. Based on the global deformations dx and dy which are provided by the photogrammetry measurement system, the shear crack opening w , the parallel crack shift v and the angular change of the shear reinforcement α (Fig. 6) were calculated.

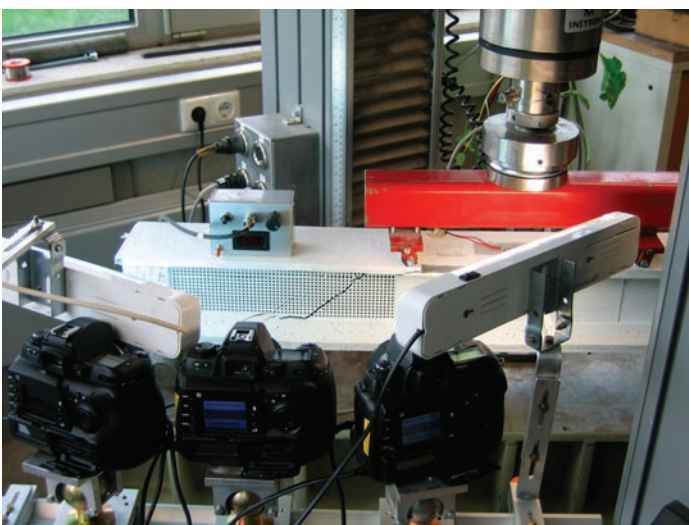


Figure 5: Photogrammetry measurement system

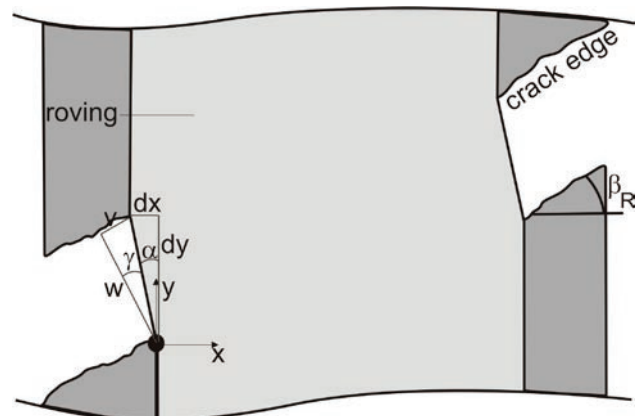


Figure 6: Shear crack geometry

The first well-known model for the description of the bearing capacity of shear reinforced beams is the truss model derived by Mörsh consisting of 45°-inclined compression struts and vertical tension elements simulating the shear reinforcement. The bearing capacity of the truss depends on the amount and strength of the shear reinforcement and is limited to the strength of the compression struts. From comparison with experimental results it is well known that this model underestimates the shear capacity particularly of beams with low shear reinforcement ratios. Therefore, in contemporary enhanced models the shear capacity of reinforced beams is composed of a truss contribution and a concrete contribution, which is governed by the bearing capacity of the compression zone. Other models take into account that the strut inclination varies, which is explained by friction forces at the shear crack edges and an aggregate interlock. Actual investigations demonstrated that the influence of the crack friction forces on the shear capacity is low because at failure loads the appearing shear crack width does not allow for the transfer of shear stresses across the cracks. Therefore, a model has been derived consisting of a truss model and a concrete contribution, which is in good agreement with test results^[7]. An important factor for the shear strength of textile-reinforced beams is the mechanical reinforcement ratio ω_E , calculated from equation (8):

$$\omega_E = \frac{a_{tw} \cdot E_{fil}}{b_w \cdot E_c} \quad (8)$$

where a_{tw} is the cross-sectional area of the shear reinforcement

E_{fil} is Young's modulus of the reinforcement

b_w is the thickness of the web

E_c is Young's modulus of the concrete.

In investigations on beams reinforced with steel stirrups a significant influence of ω_{ct} on the shear crack angle $\beta_{r,exp}$ has been detected, especially for low reinforcement ratios ($\omega_{ct} < 1.5\%$), where an increasing ω_{ct} leads to steeper shear cracks^[13]. However, due to the relatively high shear reinforcement ratio in the tests on TRC beams, no dependency could be detected. Here the average value of the shear cracks amounted to about 45°.

In order to estimate the effect of shear crack friction, the crack width w and the relative displacement of the crack edges v were calculated from the photogrammetry measurement data as explained above. The average shear crack width at failure amounted to about 0.25 mm, so that due to the small maximum grain size of 0.6 mm only little shear friction can be expected. This means that the shear crack angle $\beta_{r,exp}$ corresponds to the compression strut inclination.

As well as the knowledge of the strut inclination, the tensile strength of the shear reinforcement is required to determine the bearing capacity of the truss. Therefore the deviation α of the shear reinforcement in the crack had to be known to calculate the effective tensile strength of the rovings in the web. The tests revealed that the values for α were in the range 12–25° depending on the reinforcement ratio and the fibre material. Higher shear reinforcement ratios lead to smaller and more convenient angles α . A comparison with the results of the tensile tests with inclined reinforcement (Fig. 1) leads to the conclusion that the loss of strength due to the deviation α is significant, as the exemplary calculation of the reduction factor $k_{0,\alpha}$ for $\alpha = 25^\circ$ confirms:

$$k_{0,\alpha} = 1 - 25^\circ/90^\circ = 0.72$$

In addition, the tests revealed that the horizontal reinforcement of the web is important for the calculation of the truss capacity. Since the deviation of the longitudinal reinforcement is much higher (for $\alpha = 25^\circ$ the corresponding deviation of the horizontal rovings is about 65°), the resulting tensile strength amounts only to about 15–30% of the axial strength.

Based on the available data for the shear crack angle and deformations of the shear area in the tests, the tensile strength of the truss can be calculated:

$$V_{F,exp} = (a_{tw,v} \cdot f_{t,res,v} + a_{tw,h} \cdot f_{t,res,h}) \cdot z \cdot \cot \beta_r \cdot \cos \alpha \quad (9)$$

where $a_{tw,v}$ is the cross-sectional area of the vertical shear reinforcement

$a_{tw,h}$ is the cross-sectional area of the horizontal shear reinforcement

$f_{t,res} = k_1 \cdot k_{0,\alpha} \cdot f_{fil}$ is the resultant strength of the reinforcement with k_1 from equation (1) and $k_{0,\alpha}$ from equation (2)

z is the inner lever arm.

A comparison of the experimental truss contribution $V_{F,exp}$ with the failure loads of the tests clarifies that for low reinforcement ratios ω_{ct} the shear capacity is not completely covered, proving the existence of an additional load-bearing mechanism (Fig. 7). This is the concrete contribution, which can be explained by the shear capacity of the compression zone^[13]. The decreasing influence of the concrete contribution with increasing mechanical reinforcement ratio ω_{ct} is explained by the weakness of the concrete contribution compared to the increasing stiffness of the truss.

Further investigations into the bearing capacity of the concrete compression struts revealed that the strength of the concrete has to be reduced compared to ordinary stirrup-reinforced concrete. The reason is the appearance of transversal tensile stresses due to the weakness of the fibre material^[9]. Therefore only about 40% of the shear capacity calculated with the model described in Reference [13] has been achieved in the tests with a failure of the compression strut. Based on the tests, the shear capacity of TRC beams can be described by a truss contribution V_F and a concrete contribution $V_{c,f}$ which is mainly influenced by the load-bearing capacity of the compression zone (Fig. 8).

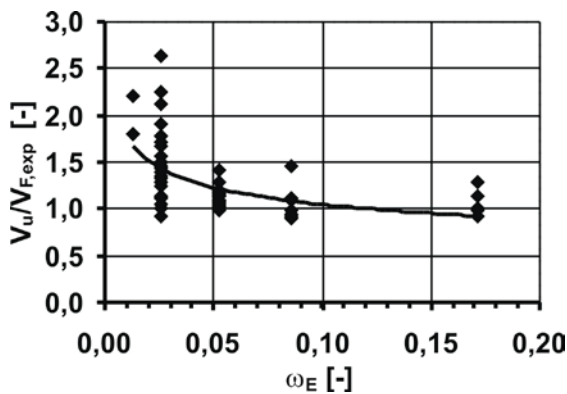


Figure 7: Ratio between shear capacity of the tests and truss contribution

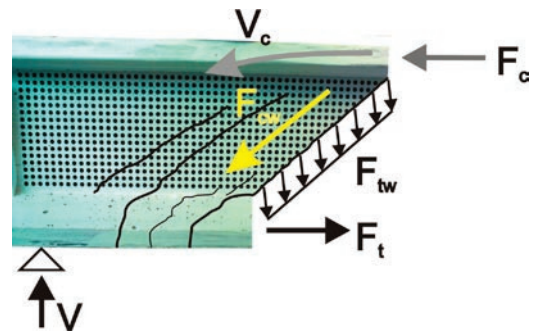


Figure 8: Shear mechanisms

Based on the described results of the investigations, a design model has been derived. According to the model described in Reference [13] the shear capacity V consists of a truss contribution V_F and a concrete contribution $V_{c,f}$. In order to consider the effect of the mechanical reinforcement ratio ω_{ct} , the factor κ_f is established.

$$V = V_F + \kappa_f \cdot V_{c,f} \quad (10)$$

The truss contribution consists of the shear resistance of the shear reinforcement and the concrete compressive strut, in which the smaller value is decisive.

$$V_F = \min \left\{ \begin{array}{l} (a_{fw,v} \cdot f_{t,res,v} + a_{fw,h} \cdot f_{t,res,h}) \cdot z \cdot \cot \beta_r \cdot \cos \alpha \\ 0,3 \cdot f_{cm} \cdot b_w \cdot z / (\cot \beta_r + \tan \beta_r) \end{array} \right. \quad (11)$$

The shear crack angle β_r depends mainly on the mechanical shear reinforcement ratio ω_{ct} and the normal stresses σ_x :

$$\text{Cot } \beta_r = 1.1 - 0.55 \sigma_x / f_{ctm} \leq 2.15 \quad (12)$$

The concrete contribution can be calculated as the shear strength of the unreinforced element according to the German standard DIN 1045-1^[14] to

$$V_{c,f} = 0,158 \cdot \beta \cdot \eta_1 \cdot \kappa \cdot \left(100 \cdot \rho_l \cdot \frac{\sigma_{tex}}{f_{yk}} \cdot f_{cm} \right)^{1/3} \cdot b_w \cdot d \quad (13)$$

where $\eta_1 = 1,0$ is for normal concrete

$$\kappa = 1 + \sqrt{\frac{200}{d}} \quad \text{is the scale factor}$$

d is the distance between reinforcement and edge of compression zone

$$\rho_l = \frac{A_r}{b_w \cdot d} \leq 0,02 \quad \text{is the longitudinal reinforcement ratio.}$$

As described above, the concrete contribution depends on the mechanical reinforcement ratio ω_{ct} (equation (8)). This effect is considered with the combination factor κ_f :

$$\kappa_f = 1 - 17\omega_E \geq 0 \quad (14)$$

Summary and conclusions

The load-bearing behaviour of TRC is influenced by material properties and the amount and alignment of the textile reinforcement. The design models known from steel-reinforced concrete cannot be applied without additional considerations. However, design models for the tension, bending and shear strength of TRC elements have been derived by analogy with known models for steel-reinforced concrete. Therefore, extensive test series have been carried out.

The bond behaviour of the textiles is of particular importance. The fibre material as well as the binding and the cross-section of the roving significantly influence the bond performance. Deviations between the direction of the tension forces and the direction of the rovings cause a loss of strength mainly initiated by the actions on the filaments at the crack edges. The assumption that the loss of strength grows linearly with increasing angle between loading and roving direction results in good accordance with test results.

The bending capacity of TRC elements can be calculated analogous with steel-reinforced concrete with an additional factor considering the effects of the curvature of the beam. The shear capacity of beams made of TRC cannot be described by a pure truss model. An additional concrete contribution exists which is the capacity of the concrete compression zone. For the calculation of the truss contribution, the angular change of the shear reinforcement has to be considered.

It should be borne in mind that the dimensioning models which are introduced in this paper are based on test results with the described AR-glassfibre and carbon fabrics and possibly have to be adapted to changing material properties. Further investigations are required to confirm the presented results and to provide a broad basis for a general design concept for TRC-elements.

Acknowledgement

The authors thank the Deutsche Forschungsgemeinschaft (DFG) in the context of the Collaborative Research Center 532 'Textile Reinforced Concrete – Development of a new technology' for its financial support.

References

1. Hegger, J., and Voss, S. Textile reinforced concrete façades. Concrete Structures: the challenge of creativity, Proceedings of the fib symposium, Avignon, France, 2004, 168-169 and cd-rom.
2. Schneider, H. N., Bergmann, I. and Schätzke, C. Leichte Betontragwerke. Detail, 2004; S, 844–854.
3. Roye, A. and Gries, T. Tensile behavior of rovings, textiles and concrete elements – possible to compare directly? Proceedings of the Third International Conference on Composites in Construction (CCC2005), Lyon, France, 2005; 1147–1154.
4. Brameshuber, W., Brockmann, T. and Banholzer, B. Material and bonding characteristics for dimensioning and modelling textile reinforced elements. Materials and Structures.
5. Ohno, S. and Hannant, D.J. Modelling the stress–strain response of continuous fiber reinforced cement composites. ACI Materials Journal, Vol. 91, No. 3, 306–312.
6. Hegger, J. and Voss, S. Tragverhalten von Textilbeton unter zweiachialer Beanspruchung. Proceedings of the Second Colloquium on Textile Reinforced Structures (CTRS2), Dresden, 29 September to 1 October 2003, S, 313–324.
7. Hegger, J. and Voss, S. Textile reinforced concrete – bearing behaviour, design, applications. Proceedings of Third International Conference Composites in Construction (CCC2005), Lyon, France, 2005, 1139–1146.
8. Hegger, J., Will, N., Bruckermann, O. and Voss, S. Load-bearing behaviour of textile reinforced concrete. Materials and Structures.
9. Molter, M. Zum Tragverhalten von Textilbewehrtem Beton. PhD thesis, RWTH Aachen University, Germany, 2005.
10. Jesse, F. Load Bearing Behaviour of Filament Yarns in a Cementitious Matrix. PhD thesis, TU Dresden, Germany, 2005.
11. Voss, S. Tragverhalten und Bemessung von Bauteilen aus Textilbewehrtem Beton. Beton- und Stahlbetonbau, Vol. 100, S. 2, Tagungsband Doktorandensymposium 45. Forschungskolloquium des DAfStb, S. 215–218.
12. Lange, J., Benning, W., Schwermann, R. and Görtz, S. Flächenhafte Deformations- und Rissanalyse an textilbewehrten Betonbauteilen mittels Photogrammetrie. Proceedings of the GESA-Symposium 2005, VDI-Berichte 1899, S. 241–251, VDI Verlag, Düsseldorf, 2005, ISBN 3-18-091899-3.
13. Görtz, S. Shear Cracking Behavior of Prestressed and Nonprestressed Beams of Normal and High Performance Concrete. PhD thesis, RWTH Aachen University, Germany, 2004.
14. DIN-1045-1, 2001, Tragwerke aus Beton, Stahlbeton und Spannbeton, Teil 1: Bemessung und Konstruktion.
15. [Heg06a] Hegger, J. and Voss, S. Design methods for textile reinforced concrete under bending and shear loading. Proceedings of the 2nd International fib Congress, June 2006, Neapel.